to harmonics of the electron cyclotron frequency and in the vicinity of the upper hybrid frequency. Ground based stations detect only those emissions which have high enough frequencies to pass across the dense ionosphere or leak through ionospheric density holes to reach the ground. The interpretation of these emissions is still unclear. Two possibilities arise. The first one is based on the cyclotron-maser mechanism acting now at relatively low altitudes in ionospheric density depletions (Weatherwax et al., 1995), the latter having been detected from ground based density measurements (Shepherd et al., 1998). It can act only in local plasma cavities. The second explanation is based on the double resonance mechanism when the upper hybrid frequency matches with the second or any higher harmonic of the cyclotron frequency. It thus works under the opposite conditions of high plasma densities. In this case the emission is narrowband and located in a very definite altitude depending on the ionospheric plasma density. It is possible that both mechanisms are at work in different places.

4.3.3.5 VLF Saucers

Perhaps the most conspicuous of the plasma waves in the downward current region is a type of electrostatic whistler emission known as a VLF saucer. VLF saucer emissions were among the first radio-wave features observed in the auroral zone (Smith et al., 1966; Gurnett, 1966) and since have been established as a common characteristic (James, 1976). The phenomenon is identified by a V-shaped or saucer-shaped appearance in a time-frequency-power spectrogram of wave electric fields in the kilohertz frequency range. Such V-shaped structures are seen over a range of time (or distance) scales ranging from less than a second (< 5 km) to hundreds of seconds (> 1000 km).

The saucer- or V-shape comes from propagation properties of quasi-electrostatic whistler waves. The lowest frequency emissions have a group velocity nearly parallel to the ambient magnetic field. Higher frequency, quasi-electrostatic whistler emissions have an oblique group velocity; the higher the frequency, the larger the angle from **B**. (We saw this already in our discussion of VLF whistler hiss; see Figure 4.28.) Thus, as a satellite passes over a small source region, it detects the higher frequencies farther away from flux tube of the source and the lowest frequencies as it passes over the flux tube of the source.

One of the most intriguing features of VLF saucers is the small physical size of the source regions that are inferred from the observations. Source sizes are as small as 0.5 km in latitude and less than 10 km in altitude (James, 1976). Such small source regions require strong, rapid wave growth. James (1976) postulated an instability from cold (< 5 eV), dense, upgoing ionospheric electrons carrying the downward or return current in the auroral zone impinging upon a warm magnetospheric population. At the time of this theory, no electrons had been detected with VLF saucers; the cold ionosphere electrons were thought to be too low in energy to be detectable by the satellite instruments. Over a decade later, the Viking satellite

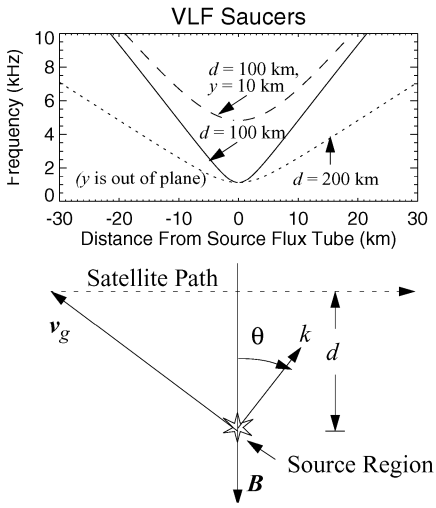

Figure 4.42. The top box shows the relation between the frequency and horizontal distance between the satellite and the source flux tube. The solid trace is the peak in the wave spectra from a point source as measured by a satellite 100 km above the source region. The dotted trace is from a point source 200 km below the satellite, and the dashed trace is 100 km below the satellite and 10 km out of the plane defined by the satellites's path and the magnetic field. The V- or saucer-shaped time-frequency-power spectrograms of electric field waves comes from the propagation characteristics of quasi-electrostatic whistlers. The bottom box shows the relation between the wave vector and group velocity for a saucer. From Ergun et al. (2001).

detected upgoing electrons associated with VLF saucers in several events, and verified that the majority of events were in the downward current region (Lonnqvist et al., 1993). Observations from the FAST satellite subsequently demonstrated that a majority of the VLF saucer sources were on flux tubes carrying intense, upgoing energetic electron fluxes.

A close examination of the VLF saucer wave spectra shows that intense broadband bursts are a frequent phenomenon at the vertex (or source flux tube) of VLF saucers (Lonnqvist et al., 1993). Subsequently, FAST observations revealed that these broadband bursts represent a series of solitary structures that have been identified as electron phase-space holes (Ergun et al., 1998c,d) indicating that electron phase-space holes are traveling upward on the same flux tubes as the VLF saucer source.

Properties. Figure 4.42 demonstrates how wave spectra vary with source location and size. The traces are examples of ideal power-frequency-distance (or time) spectrograms from point source locations. The solid trace is from a point source 100 km in altitude below the spacecraft as measured at the vertex. The plasma con-

ditions for all the examples have an electron density n_e of 20 cm^{-3}, a constant magnetic field B at 10^4 nT, and a homogenous H^+ plasma. The trace forms a 'V' in the spectrogram with a low-frequency cutoff at the lower hybrid frequency. The dotted trace displays the expected wave spectrogram from a point source 200 km below the spacecraft. The 'V' is less steep but otherwise shows the same low-frequency cutoff. Comparing these two traces demonstrates how the source size can be determined. The extent of the source in altitude determines the bandwidth of the spectra at the higher frequencies (far from the vertex), but does not dramatically change the spectra at the vertex. Thus, one determines the location and extent in altitude of the source region by examining spectra at higher frequencies far from the saucer vertex.

The dashed trace in Figure 4.42 illustrates the effect of an out-of-plane displacement of the source region. The source is 100 km below the spacecraft but 10 km out of the plane defined by the spacecraft path and magnetic field. In the case of an auroral satellite traveling in the north-south direction, the displacement would be in longitude. When compared to the solid trace, the dashed trace shows the greatest change near the vertex. It has a cutoff at a significantly higher frequency because the minimum propagation angle is non-zero. Farther from the source, that is, in horizontal distance along the spacecraft track, the effect of the out-of-plane displacement of the source is less pronounced. Thus, one determines the longitudinal position and size by examining spectra near the saucer vertex. Unfortunately, broadband emissions from electron phase-space holes at the vertex often complicate such an analysis.

Observations. Figure 4.43 shows a FAST observations of a VLF saucer. The top panel displays the DC electric field signal along the path of the spacecraft (nearly southward) and perpendicular to the ambient magnetic field. The signal is negative beginning at 00:03:25 UT and then shifts to positive at 00:03:30 UT. This signature is that of a diverging electric field structure which implies a downward parallel electric field is on the flux tube of the spacecraft at a lower altitude (see Section 4.2). Panel (b) displays the mostly east-west perturbation magnetic field signal (δB); a model magnetic field has been subtracted. The slope of the magnetic field signal indicates a current, assuming a sheet-like structure. A negative slope implies an upward current and a positive slope implies a downward current. The region of interest (00:03:25 UT to 00:03:35 UT) has a strong positive slope indicating a downward current of $\sim 2\ \mu A\ m^{-2}$.

Panel (c) displays the electric field spectral power density in the 0-16 kHz range. The dominant feature is a complex, multiple-arm, VLF saucer with the vertex at 00:03:30 UT. The vertical features in the plot (e.g., 00:03:25 UT, 00:03:29.5 UT, 00:03:45.5 UT) are bursts of broadband electrostatic noise. Panel (d) displays the electron differential energy flux (color) as a function of energy (vertical axis) and panel (e) displays the electron differential energy flux as a function of pitch angle.

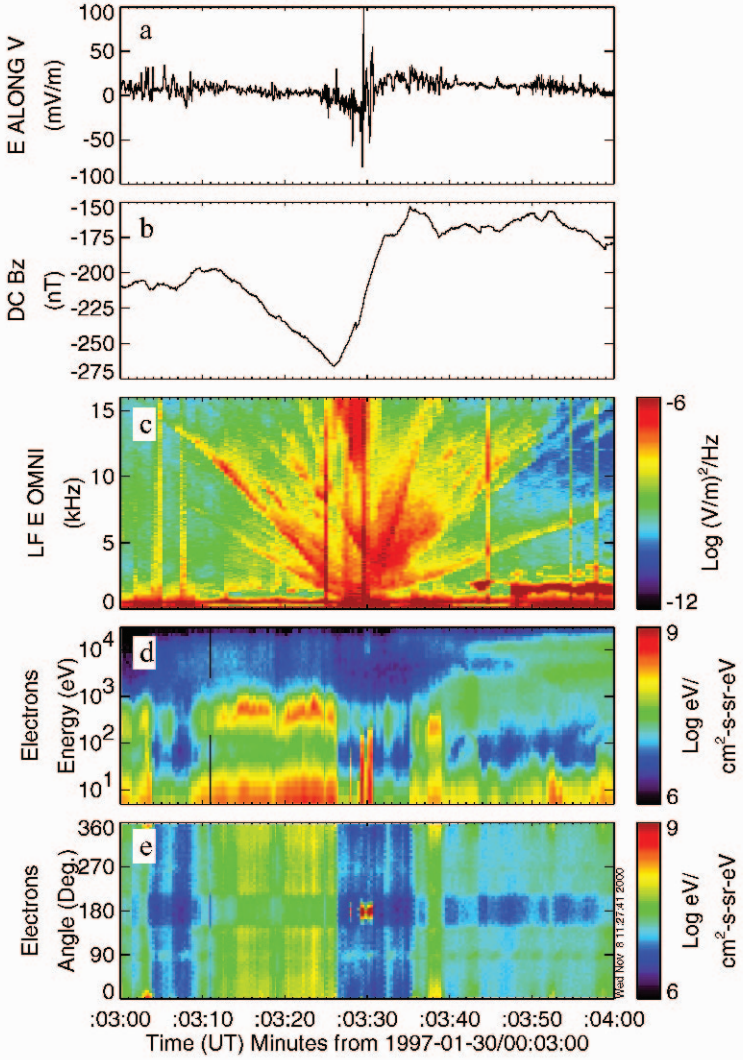

Figure 4.43. (a) The perpendicular electric field in the spin plane and nearly along the spacecraft path (mostly south). (b) ΔB along the spacecraft spin axis (mostly west) and normal to the spacecraft velocity. A negative slope indicates upward current; a positive slope indicates downward current. (c) The electric field spectral power density summed over all directions. (d) Electron differential energy flux versus energy, and (e) versus pitch angle. From (Ergun et al., 2001).

Downgoing electrons are at 0° and 360° and upgoing electrons are at 180°. During most of the 60 s period, the electron fluxes were traveling predominantly earthward. At the vertex of the VLF saucer, however, intense fluxes of highly field-aligned, ~ 100 eV electrons were traveling upward. Figure 4.43 displays a clear example in

which the VLF saucer source is associated with upgoing electron fluxes that were accelerated by a parallel electric field.

The electric field spectral power density reveals multiple VLF sources. There appear to be at least 16 distinct arms in the VLF saucer. The slopes and bandwidths of the arms provides information on the individual source sizes and locations. The narrow bandwidth (~ 40 Hz) of the arms far from the source indicates that the sources are limited to at most ~ 10 km extent in altitude and in latitude.

The slopes of the arms indicate the distance of source from the spacecraft. Distances range from ~ 100 km to over 1000 km. The vertices of the arms map from 00:03:25 UT to 00:03:35 UT, during which time the spacecraft traversed $\sim$50 km, so the individual sources may be dispersed over this region in latitude. The size of the nearest sources are less than $\sim$2 km in latitude. The bandwidth of the arms increases near the vertex (at lower frequencies), indicating a finite longitudinal size. Because of the multiple arms and the broadband electrostatic noise (vertical features), the longitudinal size cannot be determined for all of the arms.

The above observations support many of the conclusions drawn from the ISIS 2 data (James, 1976) and Viking measurements (Lonnqvist et al., 1993). The energy source appears to be from upgoing electron beams. The source regions are confined in both latitude and altitude to less than $\sim$10 km.

4.4 Time-Dependent Alfvénic Processes

Electromagnetic energy is transmitted along magnetic field lines by shear Alfvén waves when the time variability of the coupled magnetosphere ionosphere system contains power at frequencies matching or exceeding the fundamental frequency of the field line eigenmode – the frequency of a standing Alfvén wave with one-half parallel wavelength extending between the northern and southern ionosphere. Basic properties of shear Alfvén waves are described in Section 3.4, including their interaction with the ionosphere. Here we consider in situ observations of Alfvén waves and associated auroral phenomena in the ionosphere and lower magnetosphere. Observed properties depend on the frequency spectrum and transverse structure of the Alfvénic fluctuations, and on whether their source is transient in nature or quasi-harmonic. The observational signatures are also influenced by measurement effects in the lower magnetosphere, as space-time aliasing (Doppler shifting) resulting from the rapid motion of the (satellite) measurement platform across field lines is always present to some degree.

The effect of a simple Alfvén wave on the ambient medium is to induce a reversible sloshing motion of ions which carry the wave polarization current and electrons which carry the wave field-aligned current. The density perturbation accompanying the Alfvén wave is generally weak. When an Alfvén wave develops a parallel electric field, which occurs at small transverse wavelengths, it exchanges momentum and energy with the medium and can deposit substantial energy in the form of plasma heating and field-aligned electron beams. This irreversible con-